

Optimization of SERS Sensing With Micro-Lensed Optical Fibers and Au Nano-Film

Karolina Milenko[✉], Silje S. Fuglerud[✉], Astrid Aksnes, Reinold Ellingsen, and Dag R. Hjelme

Abstract—We present the fabrication and characterization of optical fiber reflection probes based on surface-enhanced Raman scattering (SERS) and micro-lensed multimode fibers. For the SERS substrate, a nano-sphere lithography method is used. Comparison of SERS measurements with three different fiber probe configurations is presented. The proposed optimized structure shows a five times increase in SERS signal for dried Rhodamine 6G (R6G) and two times for aqueous R6G in comparison to a standard reflection configuration. Measurements of different concentrations of R6G in a water solution with a limit of detection (LOD) equal to 10^{-7} M are demonstrated.

Index Terms—Fiber optics, nanoparticles, nanophotonics, optical sensors, Raman scattering.

I. INTRODUCTION

SURFACE-ENHANCED Raman scattering is orders of magnitude more sensitive than normal Raman scattering, allowing for single molecule detection [1]. In SERS, the electromagnetic field is enhanced through the excitation of localized surface plasmons of metallic nanostructures [2], [3]. Usually, SERS detection is performed by placing the sample on a nanostructured substrate in a Raman microscope, limiting the applications to a laboratory environment. However, in the last decade a combination of SERS and optical fibers has emerged as a very attractive sensing platform, enabling ultrasensitive remote sensing with optical fibers [4], [5].

Different approaches for the fabrication of nano-structures at the end-facet of optical fibers have been presented, such as laser-induced nano-particles synthesis [6], [7], focused ion beam [8] and nano-sphere lithography [9]–[11]. Typically, the coated cleaved fiber end is used both for the excitation and collection of the SERS, since this configuration provides the simplest

arrangement. However, in this type of sensor the excited SERS has to be collected through the layer of the SERS substrate. This lowers the collection efficiency and for that reason the sample is often dried before the measurements [12], preventing real-time continuous detection applications. Continuous monitoring can be crucial for many applications, such as glucose monitoring in diabetic patients [13].

In this paper, we propose a new configuration of SERS reflection probes, where a micro-lensed optical fiber (MLF) is used in combination with a gold film over nano-spheres (AuFON) SERS substrate. By introducing an MLF, the collection efficiency can be enhanced, and therefore higher sensitivity can be obtained. Previously, we demonstrated an MLF trans-reflectance probe for SERS measurements of Rhodamine 6G (R6G), where two MLF fibers were used, one for excitation and one for collection of SERS [14]. Here, we demonstrate the optimization of the MLF diameter and the MLF-SERS substrate distance in a reflection configuration, to maximize the collected SERS for both dried and liquid R6G samples. Optimization of the SERS substrate is beyond the scope of the paper. The probe design is applicable to other SERS substrates; however, AuFON substrates are attractive in the sense that they are highly reproducible, robust, and cost-effective.

II. EXPERIMENTAL

A. Fabrication

The AuFON SERS structure was fabricated using $1\text{ }\mu\text{m}$ monodisperse polystyrene microspheres (Polybead Microspheres, Polysciences Ink) and a multimode (MM) fiber with $200\text{ }\mu\text{m}$ core and $220\text{ }\mu\text{m}$ cladding diameter (FT200EMT, Thorlabs). The nano-sphere lithography method based on self-assembly was employed [11], [15], [16]. First, polystyrene microspheres mixed with ethanol (1:2) were slowly deposited on a water-air interface through a plasma treated cover glass slide immersed in the water. When a closely packed monolayer suspension of spheres was created, the cleaved MM optical fiber was immersed in the water and pulled through the microspheres layer. This resulted in the end-facet of the fiber being covered with a packed monolayer of micro-spheres.

Next, the treated fiber was mounted vertically in a Pfeiffer Electron Beam Evaporator (NTNU, NorFab) and coated with 100 nm of gold. Figure 1 shows the SEM picture of the fabrication end result. Closer inspection of the AuFON reveals a gold surface substructure roughness in the range of 10 to 60 nm (Fig. 1b). A fusion splicer (Fujikura FSM-100P) was used to

Manuscript received October 1, 2019; revised November 10, 2019; accepted December 3, 2019. Date of publication December 9, 2019; date of current version April 1, 2020. This work was supported in part by the Research Council of Norway for the Double Intraperitoneal Artificial Pancreas (Centre for Digital Life Norway) under Project 248872 and in part by the Norwegian Micro- and Nano- Fabrication Facility, NorFab under Project 245963/F50. The work of S. S. Fuglerud was supported by the Central Norway Regional Health Authority under Project 46055510. (*Corresponding author: Karolina Milenko*)

K. Milenko, A. Aksnes, R. Ellingsen, and D. R. Hjelme are with the Department of Electronic Systems, Norwegian University of Science and Technology, 7491 Trondheim, Norway (e-mail: karolina.milenko@ntnu.no; astrid.aksnes@ntnu.no; reinold.ellingsen@ntnu.no; dag.hjelme@ntnu.no).

S. S. Fuglerud is with the Department of Electronic Systems, Norwegian University of Science and Technology, 7491 Trondheim, Norway, and also with the Department of Endocrinology, St. Olav's University Hospital, 7030 Trondheim, Norway (e-mail: silje.fuglerud@ntnu.no).

Color versions of one or more of the figures in this article are available online at <https://ieeexplore.ieee.org>.

Digital Object Identifier 10.1109/JLT.2019.2958128

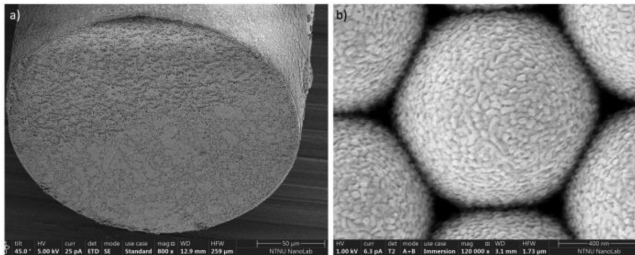


Fig. 1. SEM image of AuFON structure fabricated at the end-facet of MM optical fiber (a) polymer spheres diameter 1 μm , gold layer 100 nm thickness. (b) Close-up of the Au coated polystyrene microspheres.

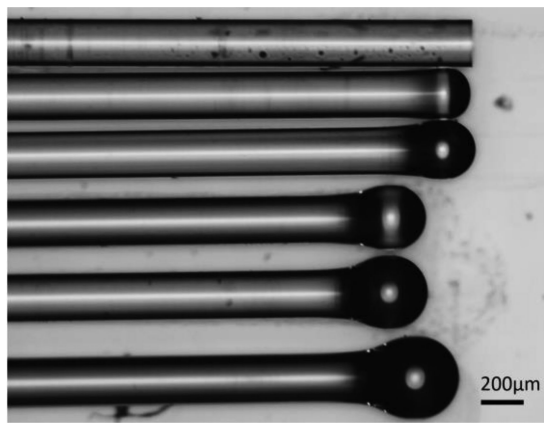


Fig. 2. The 220 μm MM fiber and fabricated micro-lensed fibers (MLF) with diameters 235, 270, 300, 335, and 375 μm .

fabricate five spherical-shaped MLF with lens diameters 235, 270, 300, 335, and 375 μm (Fig. 2). The cleaved end of the MM was melted for a chosen time span, while being rotated around its own axis, limiting the influence of gravity. The fabrication procedure was of high repeatability resulting in symmetrical shaped lens formation with a very low concentricity error.

Rhodamine 6G (R6G, Sigma-Aldrich) diluted to different concentrations in ultrapure water (Millipore) was used for the SERS measurements.

B. Experimental Setup

For the SERS reflection measurements, a 785 nm fiber-coupled laser diode (LMFC-785-PLR500, Ondax) with 63 mW power, was launched into a dichroic beam splitter (LPD02-785RU-25, Semrock) through a laser line filter (FL780-10, Thorlabs). A notch filter was used to block the laser light (NF785-33, Thorlabs) before the detection with a QE Pro Raman Spectrometer (Ocean Optics) (Fig. 3a). Three different configurations of the SERS optical fiber reflection probes with AuFON structures were fabricated and tested. The first configuration was a simple reflection probe, a common configuration used for SERS fiber measurements [7]–[9]. Here the light is coupled into the AuFON coated MM fiber and SERS is collected with the same fiber (Fig. 4 a-1). In the second configuration, the excitation and collection is done with a cleaved MM fiber mounted at a distance from a AuFON structure (Fig. 4 a-2). The third configuration

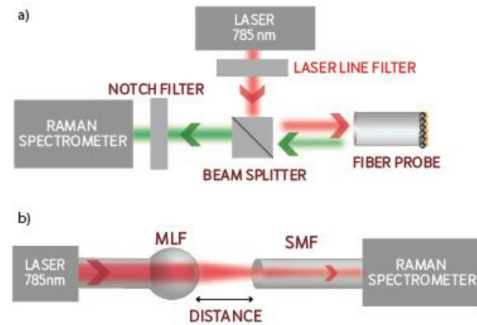


Fig. 3. Schematic diagram of the experimental setups. (a) SERS in a reflection configuration. (b) Transmission measurements.

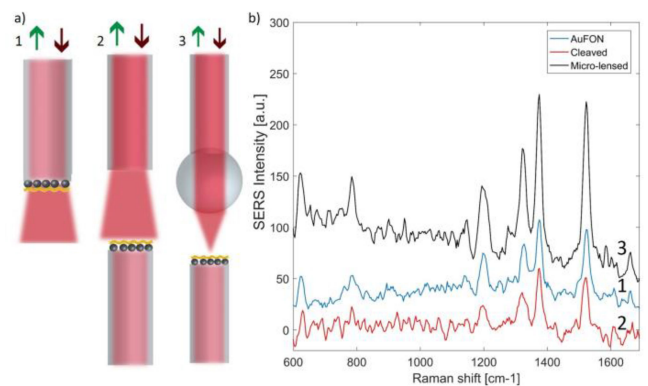


Fig. 4. (a) Three configurations of SERS fiber probes. 1- reflection with AuFON coated MM fiber, 2- excitation and collection of SERS with a cleaved MM fiber, 3- excitation and collection of SERS with a micro-lensed MM fiber with 375 μm diameter. (b) Corresponding SERS measurements.

used an MLF for both the excitation and collection (Fig. 4 a-3). Here, the AuFON structure was immersed for 15 min in an R6G solution with a 1 mM concentration, removed, and dried for 30 min.

For the MLF focal point measurements, a simplified setup with the 785 nm laser diode and the QE Pro Raman Spectrometer was used (Fig. 3b). A single mode fiber (SMF) was aligned with the MLF at the point of maximum transmission intensity and pulled back using a 3D micro-stage (Thorlabs). The transmitted light was measured as a function of the distance between the SMF and the MLF.

III. RESULTS

A. Probe Configurations for SERS Measurements

The three configurations of the optical fiber reflection probe were tested using the same AuFON substrate with dried R6G.). The collection fibers and the AuFON coated MM fiber were aligned using 3-axis translation stages (MBT616D, Thorlabs) while monitoring the SERS signal for the maximum response. The results of the SERS measurement, using 1 s integration and 10 spectral averages, are presented in Figure 4b. The SERS intensity for the first and second configuration is comparable, 60 counts for the 1375 cm^{-1} peak height above the background

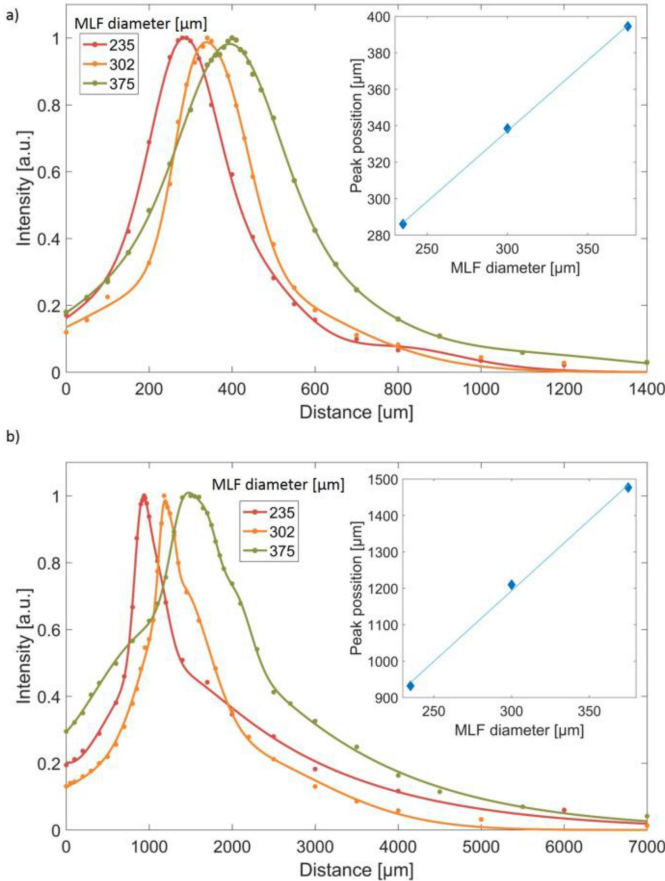


Fig. 5. Normalized, measured transmitted intensity as a function of distance from the micro-lensed fiber edge (a) in air (Inset: peak position vs. MLF diameter) and (b) in water (Inset: peak position vs. MLF diameter).

level. For the third configuration, where the MLF was used, the peak height is 164 counts, which is 2.7 times higher than in the two first configurations. Accordingly, using an MLF for both excitation and collection improved the SERS signal significantly and increased the sensitivity of the SERS reflection probe.

By optimizing the MLF diameter and the distance to the SERS substrate for configuration three, an additional improvement in SERS signals can be obtained, as shown in section C below.

B. MLF Characterization

As shown above, the MLF improves the excitation and collection efficiency of the generated SERS signal. In this section, the optimization of the MLF diameter will be shown for the SERS measurements of dried and aqueous R6G samples.

The strength of the measured SERS signal is determined by the focusing properties of the MLFs. To determine how the focusing properties vary with lens diameter, three MLFs with lens diameters 235, 302, and 375 μm (Fig. 2) were characterized using the setup in Figure 3b. The transmitted light was measured both in air and in water. The normalized transmissions for the different MLF diameters are shown in Fig. 5a, b. The effective focal length, defined as the distance giving maximum transmission, increases with lens diameter, consistent with theoretical calculations consistent using the paraxial geometrical ray

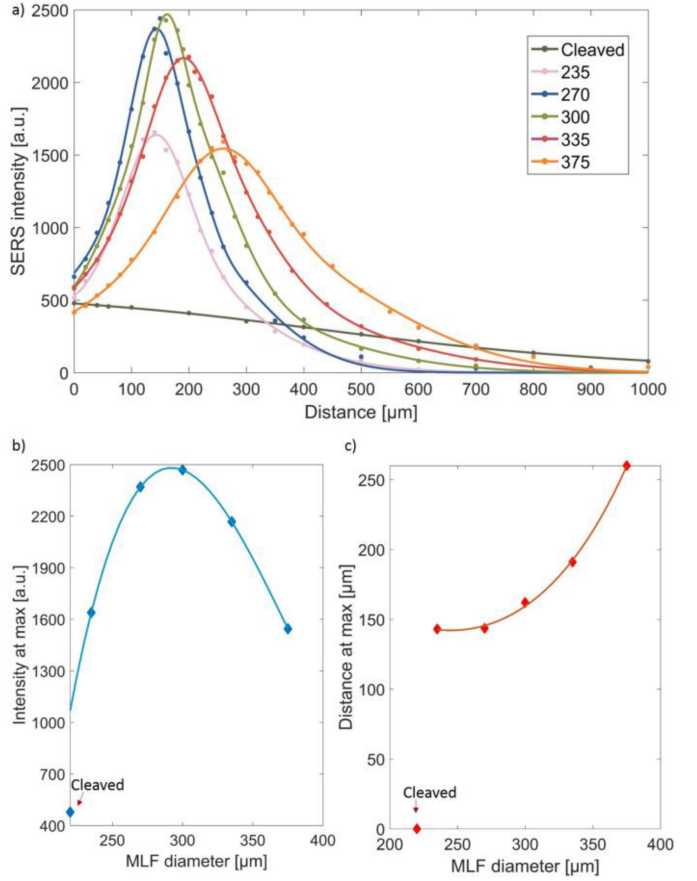


Fig. 6. SERS intensity of dried R6G in air measured in the reflection mode (a) as a function of distance of the SERS substrate from the edge of the micro-lensed fiber, (b) maximum Raman intensity vs. diameter of the micro-lens, and (c) distance at maximum SERS intensity vs. the MLF diameter.

approximation [17]. Similarly, the focal-depth (the full-width half-maximum of the normalized transmission) increases with lens diameter. Measured in air, the focal lengths are in the range 290–390 μm for the selected MLFs. The focal length measured in water is longer, in the range 900–1400 μm (Fig. 5b), due to the higher refractive index of the surrounding medium.

C. SERS Measurements

It is not given that the focal length of the MLF is the optimum distance to obtain the maximum SERS signal. It is therefore of interest to characterize the performance of the MLFs in the presence of a SERS substrate. The SERS intensity measurements were performed as function of the distance between the measuring fiber and the AuFON structure. Five MLFs with diameters 235, 270, 300, 335, and 375 μm, as well as cleaved MM fibers were used for the measurement in a reflection configuration (Fig. 4a (2–3)).

First, the SERS signal from R6G dried on the SERS substrate was measured. The maximum SERS intensity was observed when the AuFON structure was placed at a distance shorter than the measured focal distance of the specific MLF (Fig. 6a). While the excitation power density is highest with the SERS substrate placed at the focal point, the SERS signal collection efficiency

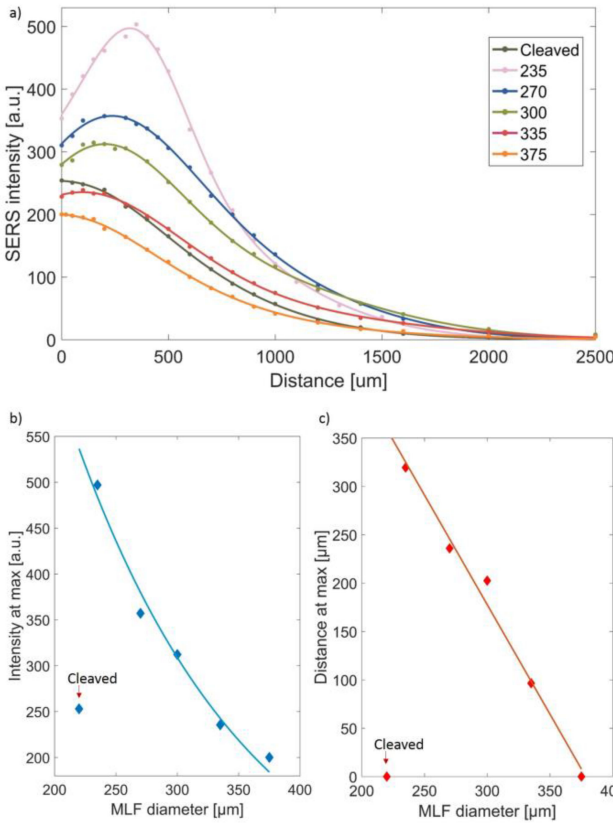


Fig. 7. SERS intensity measured in the reflection mode of R6G in aqueous solution (a) as a function of distance of the SERS substrate from the edge of the micro-lensed fiber, (b) maximum Raman intensity vs. diameter of the micro-lens, and (c) distance at maximum SERS intensity vs. the MLF diameter.

at this distance is limited by the effective aperture of the MLF, i.e., only a small fraction of the SERS angular spectrum will couple to the fiber. Moving the SERS substrate closer to the MLF will increase the collection efficiency by increasing the fraction of the angular spectrum coupled to the fiber. If the SERS substrate is too close to the MLF, the collection efficiency will decrease as the angular spectrum coupled to the fiber will be limited by the numerical aperture (NA) of the MLF (defined here as the acceptance angle at a given distance). Thus, the behavior observed in Fig. 6a is as expected. The maximum SERS intensity as a function of MLF diameter and the distance between the MLF and SERS substrate are presented in Figure 6b, c. The result for the cleaved fiber is also presented in the figures; however it was not used for the curve fitting. The measured SERS intensity is highest with the 300 μm diameter MLF (~ 2500 counts) (Fig. 6b), which is 5 times higher than the intensity measured with a cleaved fiber.

The SERS measurements were also performed for aqueous solutions of R6G. SERS intensity as a function of distance of the SERS substrate from the edge of the MLF is presented in Figure 7a. The highest SERS intensity equal to 500 counts, observed with the 235 μm MLF, was 2 times higher than with a cleaved MM fiber (Fig. 7b). Moreover, the intensity drops exponentially with increasing MLF diameter (the cleaved MMF was not included in the fitting). The maximum SERS signal

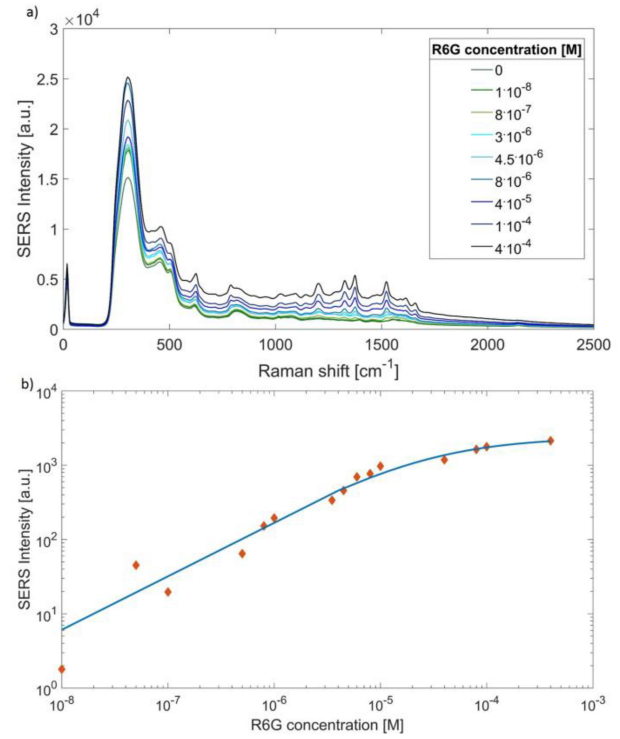


Fig. 8. (a) Raw SERS spectra of R6G in an aqueous solution with a concentration range of $1 \cdot 10^{-8} - 5 \cdot 10^{-4}$ M. (b) SERS intensity for the Raman peak at 1200 cm^{-1} as a function of the R6G concentration (red points); fitted to a Langmuir-Freundlich isotherm (blue line).

is observed at a shorter distance than the specific MLF focal length (Fig. 7c). Furthermore, the distance to the maximum SERS signal is reduced with increasing MLF diameter. This is opposite to the shift of the focal distance with increasing MLF diameter.

The maximum observed SERS for the 375 μm MLF was when the distance was equal to zero. This can be explained by the fact that the refraction at the MLF-liquid interface is very weak, such that the SERS collection efficiency limitation in most cases is dominated by the NA of the fiber, i.e., the collection efficiency is best at zero distance. Only for the largest curvature, i.e., 235 μm diameter, we have enough refraction to see significant increase in SERS signal with distance to the SERS substrate. Additionally, the distance between the collection fiber and the AuFON substrate plays an important role in the probe construction. From Figure 7c it follows that the maximum SERS intensity measured with the cleaved fiber is obtained when the fiber and SERS substrate are in contact (distance equal to 0 μm), while for the fabricated MLFs the distance increases exponentially for increasing MLF diameter and ranges from 140 to 260 μm . This allows for a sufficient volume of the sample to be placed in between the fibers, facilitating sample flow and easy probe cleaning.

D. Concentration Measurements

The 235 μm MLF found as the optimum diameter for measurements of aqueous samples was used for concentration

measurements. R6G was dissolved in water to create different concentrations in the range of 10^{-8} to 10^{-4} M. A $100 \mu\text{L}$ droplet of aqueous R6G solution was placed between and around the fibers. The sensing structure was washed with ethanol and water before each new concentration measurement to remove any residual R6G on the surfaces. The measurements were performed at room temperature, while the spectra were measured with 4 s integration time and averaged over 10 spectra.

Figure 8a shows the increase in intensity of SERS signal from R6G with increasing concentration. The signal below 200 cm^{-1} was blocked by the filter, while the strong background signal between 200 and 500 cm^{-1} was a Raman signal originating from the optical fibers used. The spectra between 1000 and 1700 cm^{-1} show the peaks related to the R6G SERS signal. Additionally, with increasing concentration we observed an increase in the fluorescent signal. Therefore, to correctly analyze the SERS intensity versus the R6G concentration, a baseline correction had to be applied [18]. A 4th degree polynomial was fitted to the minima located between the Raman peaks in the selected wavenumber region for each concentration and subtracted from the spectra [19]. The resulting intensity of the 1200 cm^{-1} peak versus the R6G concentration is presented in Fig. 8b, showing a log–log linear dependence in the concentration range 10^{-7} – 10^{-5} M, with a linear regression slope ($\alpha = \log(\text{Intensity})/\log(\text{concentration})$) equal to 0.81. For higher concentrations, saturation effects are observed, which are in agreement with the Langmuir–Freundlich adsorption model [20]. The limit of detection (LOD) is estimated to 10^{-7} M, based on the 1200 cm^{-1} peak being 3 times higher than the noise level for this concentration [21]. This result is better than previously reported by us [14] and comparable to similar SERS fiber-based devices [22]. However, by optimizing the SERS substrate and the pump power and using multivariate chemometric techniques, the LOD could be further improved.

IV. CONCLUSION

In this paper, we presented an unquestionable increase in the collected SERS signal by using MLF in comparison to a cleaved MM fiber in a SERS reflection probe. Additionally, we presented the experimental optimization of the MLF diameter and the distance between the MLF SERS substrate for the excitation and collection of SERS for dried and aqueous samples. We showed that by using the MLF in a reflection probe, we can increase the measured SERS intensity by a factor 5 for dried samples and a factor 2 for aqueous samples. Lastly, the measurements of R6G in an aqueous solution with different concentrations were presented, resulting in an LOD equal to about 10^{-7} M.

REFERENCES

- [1] K. Kneipp *et al.*, “Single molecule detection using surface-enhanced Raman scattering (SERS),” *Phys. Rev. Lett.*, vol. 78, no. 9, pp. 1667–1670, 1997.
- [2] P. L. Stiles *et al.*, “Surface-enhanced Raman spectroscopy,” *Annu. Rev. Anal. Chem.*, vol. 1, pp. 601–626, 2008.
- [3] K. A. Willets and R. P. Van Duyne, “Localized surface plasmon resonance spectroscopy and sensing,” *Annu. Rev. Phys. Chem.*, vol. 58, pp. 267–297, 2007.
- [4] S. S. Dasary *et al.*, “Gold nanoparticle based label-free SERS probe for ultrasensitive and selective detection of trinitrotoluene,” *J. Amer. Chem. Soc.*, vol. 131, no. 38, pp. 13806–13812, 2009.
- [5] C. Wang *et al.*, “Review of optical fibre probes for enhanced Raman sensing,” *J. Raman Spectrosc.*, vol. 48, no. 8, pp. 1040–1055, 2017.
- [6] J. Cao, D. Zhao, and Q. Mao, “Laser-induced synthesis of Ag nanoparticles on the silanized surface of a fiber taper and applications as a SERS probe,” *RSC Advances*, vol. 5, no. 120, pp. 99491–99497, 2015.
- [7] C. Liu *et al.*, “A surface-enhanced Raman scattering (SERS)-active optical fiber sensor based on a three-dimensional sensing layer,” *Sens. Bio-Sens. Res.*, vol. 1, pp. 8–14, 2014.
- [8] G. F. Andrade *et al.*, “Surface-enhanced resonance Raman scattering (SERRS) using Au nanohole arrays on optical fiber tips,” *Plasmonics*, vol. 8, no. 2, pp. 1113–1121, 2013.
- [9] G. Quero *et al.*, “Nanosphere lithography on fiber: Towards engineered lab-on-fiber SERS optrodes,” *Sensors*, vol. 18, no. 3, p. 680, 2018.
- [10] M. Pisco *et al.*, “Nanosphere lithography for advanced all fiber sers probes,” *Proc. SPIE*, vol. 9916, 2016, Art. no. 99161S.
- [11] M. Pisco *et al.*, “Nanosphere lithography for optical fiber tip nanoprobes,” *Light, Sci. Appl.*, vol. 6, no. 5, 2017, Art. no. e16229.
- [12] J. Zhang *et al.*, “Tapered fiber probe modified by Ag nanoparticles for SERS detection,” *Plasmonics*, vol. 11, no. 3, pp. 743–751, 2016.
- [13] I. L. Jernelv *et al.*, “A review of optical methods for continuous glucose monitoring,” *Appl. Spectrosc. Rev.*, vol. 54, no. 7, pp. 543–572, 2019.
- [14] K. Milenko *et al.*, “Micro-lensed optical fibers for a surface-enhanced Raman scattering sensing probe,” *Opt. Lett.*, vol. 43, no. 24, pp. 6029–6032, 2018.
- [15] N. G. Greenelch *et al.*, “Immobilized nanorod assemblies: Fabrication and understanding of large area surface-enhanced Raman spectroscopy substrates,” *Anal. Chem.*, vol. 85, no. 4, pp. 2297–2303, 2013.
- [16] J. C. Hulteen and R. P. Van Duyne, “Nanosphere lithography: A materials general fabrication process for periodic particle array surfaces,” *J. Vac. Sci. Technol. A, Vac., Surf., Films*, vol. 13, no. 3, pp. 1553–1558, 1995.
- [17] F. Träger, *Springer Handbook of Lasers and Optics*. Berlin, Germany: Springer, 2012, pp. 53–54.
- [18] K. H. Liland, A. Kohler, and N. K. Afseth, “Model-based pre-processing in Raman spectroscopy of biological samples,” *J. Raman Spectrosc.*, vol. 47, no. 6, pp. 643–650, 2016.
- [19] N. K. Afseth, V. H. Segtnan, and J. P. Wold, “Raman spectra of biological samples: A study of preprocessing methods,” *Appl. Spectrosc.*, vol. 60, no. 12, pp. 1358–1367, 2006.
- [20] R. Sips, “On the structure of a catalyst surface,” *J. Chem. Phys.*, vol. 16, no. 5, pp. 490–495, 1948.
- [21] A. Shrivastava and V. B. Gupta, “Methods for the determination of limit of detection and limit of quantitation of the analytical methods,” *Chronicles Young Scientists*, vol. 2, no. 1, pp. 21–25, 2011.
- [22] G. F. Andrade, M. Fan, and A. G. Brolo, “Multilayer silver nanoparticles-modified optical fiber tip for high performance SERS remote sensing,” *Biosensors Bioelectron.*, vol. 25, no. 10, pp. 2270–2275, 2010.